PhenoCam Dataset v3.0: Vegetation Phenology from Digital Camera Imagery, 2000-2023

Get Data

Documentation Revision Date: 2025-03-10

Dataset Version: 3

Summary

This dataset provides vegetation phenological observations for 738 sites across diverse ecosystems of the world (mostly North America) from 2000 to 2023. The phenology data were derived from conventional visible-wavelength automated digital camera imagery collected through the PhenoCam Network at each site. From each acquired image, RGB (red, green, blue) color channel information was extracted and summary statistics were calculated for a region-of-interest (ROI) that delineates an area of specific vegetation type. From the high-frequency (typically, 30 minute) imagery collected over several years, time series characterizing vegetation color, including canopy greenness, plus greenness rising and greenness falling transition dates, were summarized over 1- and 3-day intervals. These data products, consisting of 4805.5 site-years of observations, can be used for phenological modeling, to evaluate satellite remote sensing data products, to understand relationships between canopy phenology and ecosystem processes, to study the seasonal changes in leaf-level physiology that are associated with changes in leaf color, for benchmarking earth system models, and for studies of climate change impacts on terrestrial ecosystems. The data are provided in comma separated values (CSV), TIFF image, text, JSON, and GeoJSON formats.

This data set holds a total of 14,284 files. It contains 738 site descriptions files (in both *.txt format and *.JSON format), 2406 region-of-interest definition (ROI) files in TIFF format, 10,401 *.csv files, including ROI index files, and time series of extracted image color and greenness transitions processed to 1- and 3-day intervals, as well as time series of "camera NDVI" at 1- and 3-day intervals, and a new "simplified" data product at 1-day interval. Site locations and basic characteristics are also included in a GeoJSON file.

Figure 1. PhenoCam Network image from the Coweeta, North Carolina site. The region of interest (ROI) at the time this image was acquired was the transparent area with deciduous vegetation in the foreground.

Citation

Zimmerman, O., A.M. Young, T. Milliman, K. Hufkens, K. Ballou, C. Coffey, K. Begay, M. Fell, M. Javadian, A.K. Post, C. Schadel, Z. Vladich, D.M. Browning, C.R. Florian, M.A. Friedl, M. Moon, M.D. SanClements, B. Seyednasrollah, A.D. Richardson, M. Abraha, M. Alber, D.W. Allen, M. Apple, M.A. Arain, A.C. Axel, P.H.J. Badiou, M. Bahn, J. Baker, D. Baldocchi, S.L.J. Bayliss, N. Behrens, C.M. Beier, C.J. Bernacchi, D. Berveiller, J. Bhattacharjee, S.C. Biraud, J.J. Blais, P. Blanken, M. Bonfim, D.D. Bosch, R. Boughton, E.H. Boughton, R.F. Brown, N. Brunsell, S.P. Burns, M.S.

Carbone, B.R. Carlson, A. Carrara, M. Cavagna, W.S. Chan, J. Chen, A. Christen, N. Chrysoulakis, H. Chu, P.E. Clark, B.J. Conrad, M.R. Cortese, R.M. Crandall, E. Cremonese, H. Crepaz, F.W. Davis, D. Debinski, A.R. Desai, M. Detto, R. Diaz-Delgado, L. Duchesne, A. Dunn, K.J. Easterday, D.M. Eissenstat, T. El-madany, D.S.S. Ellum, S.K.M. Ernest, A. Esposito, E.S. Euskirchen, L. Fenstermaker, L.F. Filchev, J.M. Fill, L.B. Flanagan, B. Forsythe, J.M. Frank, A.L. Freestone, J. Gallagher, M. GarcÃ⊠a, D. Garcia-Diaz, M. Gharun, D. Gianelle, J.M. Gonet, S.C. Goslee, T. Griffis, P. Groffman, L. Gu, J. Guillemot, I.M. Halm, M. Halpin, A. Hammerle, P.J. Hanson, C.V. Hanson, Z. Harlow, K.M. Hart, C.E. Hatch, P.L. Heinrich, D. Hemming, M. Heskel, A.C. Hill, A.A. Hove, T. Hubner, D. Hui, E.R. Humphreys, P.C. Inkenbrandt, A. Jaimes-Hernandez, R. Jensen, J. Johnson, B.G. Johnson, L.S.K. Joseph, E. Keel, V.R. Kelly, K.W. King, J.W. Kirchner, P.B. Kirchner, M.A. Kline, S.H. Knox, M. Krassovski, K.L. Ladig, P.E. Laerke, O. Langvall, G. Lanthier, N.K. Lany, R. López Jiménez, G.l. Maire, H. Liu, Y. Luo, A. Manco, J. Marrs, T.A. Martin, M. Mauritz, G. McCarty, B. McNeil, F. Meier, M. Mensinger, G. Meyer, M. Migliavacca, T. Miura, B.P. Mohanty, C.E. Moore, R. Mudd, J.W. Munger, Z.E. Murrell, Z. Nesic, H.S. Neufeld, J. Norris, J. O'Connell, T.L. O'Halloran, W. Oechel, A.C. Oishi, B. Oryan, W.W. Oswald, D.M.P. Peltier, J. Perez-Quezada, T.D. Perkins, C. Phillips, M. Pizarro, D. Poursanidis, J.W.M. Pullens, P. Ramanamandimby, M.P. Rao, R.L. Ray, M.L. Reba, C. Redmond, A. Reinmann, D.A. Roberts, G.P. Robertson, M. Rodriguez-Caton, K. Rumora, B.C. Rundquist, B.R.K. Runkle, T. Sachs, E.J. Sadler, A. Saha, N.Z. Saliendra, T.S. Sankey, H. Scheifinger, L. Schmalbeck, M.R. Schuppenhauer, M.D. Schwartz, R.L. Scott, S.D. Sebestyen, D. Smale, E.M. Smith, J. Smith, O. Sonnentag, P. Stoy, S. Strachan, K. Suvocarev, D. Szutu, F. Tekinay, J.E. Thom, R.Q. Thomas, C. Trauernicht, D. Trejo, D. Tsirantonakis, A. Valero, A.K. Van den berg, M.K. Van der molen, R. Vargas, M. Vellend, J. Verfaillie, C.S. Vogel, A. Vrieling, J.J. Walker, J.R. Ward, D.A. Watts, N. Webb, P. Wetzel, S. Weyers, A.V. Whipple, C.W. Whippo, W.A. White, T.G. Whitham, C. Wille, A. Wingler, G. Wohlfahrt, S. Wolf, J.D. Wood, A.L. Woodley, J. Yang, X. Yang, G. Yenni, A.J. Zambrano-olimpo, A. Zandonai, Y. Zhang, and D. Zona. 2025. PhenoCam Dataset v3.0: Vegetation Phenology from Digital Camera Imagery, 2000-2023. ORNL DAAC, Oak Ridge, Tennessee, USA. https://doi.org/10.3334/ORNLDAAC/2389

Table of Contents

1. Dataset Overview

This dataset provides vegetation phenological observations for 738 sites across diverse ecosystems of the world (mostly North America) from 2000 to 2023. The phenology data were derived from conventional visible-wavelength automated digital camera imagery collected through the PhenoCam Network at each site. From each acquired image, RGB (red, green, blue) color channel information was extracted and summary statistics were calculated for a region-of-interest (ROI) that delineates an area of specific vegetation type. From the high-frequency (typically, 30 minute) imagery collected over several years, time series characterizing vegetation color, including canopy greenness, plus greenness rising and greenness falling transition dates, were summarized over 1- and 3-day intervals. These data products, consisting of 4805.5 site-years of observations, can be used for phenological modeling, to evaluate satellite remote sensing data products, to understand relationships between canopy phenology and ecosystem processes, to study the seasonal changes in leaf-level physiology that are associated with changes in leaf color, for benchmarking earth system models, and for studies of climate change impacts on terrestrial ecosystems.

This version 3 dataset includes a new “simplified” data format that is designed to be more accessible for most users. It also provides time series of "camera NDVI”, summarized over 1- and 3-day intervals, for the 586 sites with cameras capable of acquiring both RGB and RGB+NIR (near infrared) imagery.

Raw images for this project are published in related dataset Ballou, K. et al. 2024.

Related Publications:

Richardson, A.D., K. Hufkens, T. Milliman, D.M. Aubrecht, M. Chen, J.M. Gray, M. R. Johnston, T.F. Keenan, S.T. Klosterman, M. Kosmala, E.K. Melaas, M.A. Friedl, and S. Frolking. 2018. Tracking vegetation phenology across diverse North American biomes using PhenoCam imagery. Scientific Data 5:180028. https://doi.org/10.1038/sdata.2018.28

Seyednasrollah, B., A.M. Young, K. Hufkens, T. Milliman, M.A. Friedl, S. Frolking, and A.D. Richardson. 2019. Tracking vegetation phenology across diverse biomes using PhenoCam imagery: The PhenoCam Dataset v2.0. Scientific Data 6:222. https://doi.org/10.1038/s41597-019-0229-9

Young, A.M., T. Milliman, K. Hufkens, K. Ballou, C. Coffey, K. Begay, M. Fell, M. Javadian, A.K. Post, C. Schädel, Z. Vladich, O. Zimmerman, D.M. Browning, C.R. Florian, M.A. Friedl, M. Moon, M.D. SanClements, B. Seyednasrollah, and A.D. Richardson. 2024. Tracking vegetation phenology across diverse biomes using PhenoCam imagery: The PhenoCam Dataset v3.0. Submitted to *Earth System Science Data*.

Related Datasets:

Ballou, K. et al. 2024. PhenoCam Dataset v3.0: Digital Camera Imagery from the PhenoCam Network, 2000-2023. ORNL DAAC, Oak Ridge, Tennessee, USA. https://doi.org/10.3334/ORNLDAAC/2364

- Digital images used for the vegetation phenology analysis.

Seyednasrollah, B.,et al. 2019. PhenoCam Dataset v2.0: Vegetation Phenology from Digital Camera Imagery, 2000-2018. ORNL DAAC, Oak Ridge, Tennessee, USA. https://doi.org/10.3334/ORNLDAAC/1674

- Version 2 of this dataset

Milliman, T., et al. 2019. PhenoCam Dataset v2.0: Digital Camera Imagery from the PhenoCam Network, 2000-2018. ORNL DAAC, Oak Ridge, Tennessee, USA. https://doi.org/10.3334/ORNLDAAC/1689

- Version 2 imagery

Acknowledgments:

The development of PhenoCam has been supported by the Northeastern States Research Cooperative, the National Science Foundation, the Long-Term Agroecosystem Research (LTAR) network which is supported by the United States Department of Agriculture, the National Ecological Observatory Network (NEON) program sponsored by the National Science Foundation and operated under cooperative agreement

by Battelle, the U.S.Department of Energy, Oak Ridge National Laboratory managed by UT-Battelle, the U.S. National Park Service Inventory and Monitoring Program, the USA National Phenology Network, and the North Central Climate Science Center of the United States Geological Survey.

Refer to the PhenoCam Fair Use Data Policy at https://phenocam.nau.edu/webcam/fairuse_statement/.

2. Data Characteristics

Spatial Coverage: Multiple points mostly over North America, Europe, and other continents

Spatial Resolution: Point

Temporal Resolution: daily and three days

Temporal Coverage: 1999-12-31 to 2023-12-31

Spatial Extent: (All latitude and longitude given in decimal degrees)

Sites	Westernmost Longitude	Easternmost Longitude	Northernmost Latitude	Southernmost Latitude
Global	-158.170	172.350	71.283	-45.038

Data File Information

This data set holds a total of 14,284 files. It contains 738 site descriptions files (in both *.txt format and *.JSON format), 2406 region-of-interest definition (ROI) files in TIFF format, 10,401 *.csv files, including ROI index files, and time series of extracted image color and greenness transitions processed to 1- and 3-day intervals, as well as time series of "camera NDVI" at 1- and 3-day intervals, and a new "simplified" data product at 1-day interval. Site locations and basic characteristics are also included in a GeoJSON file.

The files can be organized by site (n=738) with up to 14 files per site (Table 1).

Table 1. File types and naming conventions.

File content	Temporal aggregation	Naming convention
PhenoCam site descriptions	-	<sitename>_meta.json
	-	<sitename>_meta.txt
Region of interest (ROI) mask	-	<sitename>_<veg_type>_<ROI_ID>_<mask_index>.tif
ROI list	-	<sitename>_<veg_type>_<ROI_ID>_roi.csv
ROI color statistics	per image	<sitename>_<veg_type>_<ROI_ID>_roistats.csv
	1-day	<sitename>_<veg_type>_<ROI_ID>_1day.csv
	3-day	<sitename>_<veg_type>_<ROI_ID>_3day.csv
Phenological transition dates	1-day	sitename>_<veg_type>_<ROI_ID>_1day_ transition_dates.csv
	3-day	<sitename>_<veg_type>_<ROI_ID>_3day_transition_dates.csv
Camera NDVI statistics	per image	<site_name>_<veg_type>_<ROI_ID>_ndvi_roistats.csv
	1-day	<site_name>_<veg_type>_<ROI_ID>_ndvi_1day.csv
	3-day	<site_name>_<<veg_type>_<ROI_ID>_ndvi_3day.csv
Simplified summary color statistics	1-day	<site_name>_<veg_type>_<ROI_ID>_simplified_1day.csv
Simplified transition dates	1-day	<site_name>_<veg_type>_<ROI_ID>_simplified_transition_dates.csv

In the file naming conventions, <**sitename**> is the name of each camera site, <**veg_type**> is a two-letter code defining the type of vegetation (Table 4), and <**ROI_ID**> is a unique identifier to distinguish between multiple regions of interest (ROI) of the same vegetation type for a given site. The <**mask_index**> is used to distinguish between multiple ROI mask files for the same site having the same *veg_type* and *ROI_ID* components.

In all files, missing data is indicated by "NA".

Data File Details

PhenoCam site descriptions

These files provide general metadata for the PhenoCam network sites included in this data set. Following general project information, site specific location, contacts, date range, and environmental and ecological characteristics are listed. Files are provide in plain text (*_meta.txt) and machine-readable JSON format (*_meta.json).

Table 2. Variables within the *meta.txt and *meta.json files.

Variable	Units	Description
last_updated	YYYY-MM-DD	the date on which the site metadata were last updated

project	-	by default, all sites are associated with the PhenoCam Network project
project_url	-	the URL of the PhenoCam project web page
fairuse_statement	-	the general PhenoCam statement on data use, acknowledgment, and redistribution
project_fairuse_url	-	the URL of the PhenoCam fairuse_statement
sitename	-	the name of the camera site, e.g. “coweeta,” used to designate all images and products associated with that site
long_name	-	a more descriptive name for each camera site
lat	degrees_north	the latitude (in decimal degrees) of the camera itself
lon	degrees_east	the longitude (in decimal degrees) of the camera itself
elevation	m	the elevation of the ground surface (m above sea level) at the camera site
contact1, contact2	-	the names and email addresses of the site representatives
active	-	“True” if new images from the site are still being added as of last_updated date; “False” if otherwise
date_start	YYYY-MM-DD	the date of the first image in the archive for this site
date_end	YYYY-MM-DD	the date of the most recent image as of the last_updated date
nimage	1	number of images in the archive for this site
site_type	-	the site class (Type I, II, or III)
ir_enabled	-	“Y” if the camera is capable of taking both visible and infrared (or visible+infrared) imagery
method	-	transfer methods to the PhenoCam server: “ftppush”= FTP: , “httppull"= pulled from an external server
utc_offset	h	difference between UTC time and local standard time at site
camera_description	-	the brand and model of the camera being used
camera_orientation	-	the compass direction in which the camera is pointing
group	-	a number of camera sub-networks
flux_data	-	“True” if eddy covariance flux measurements are being (or have been) made at the site
flux_networks	-	name of flux network if the site belongs to a network (e.g., AmeriFlux, Fluxnet-Canada)
flux_sitenames	-	site code (e.g., FLUXNET, AmeriFlux), if applicable
ecoregion	-	numeric code identifying the site’s EPA Ecoregion
MAP_site	mm	mean annual precipitation as reported by site personnel
MAP_daymet	mm	mean annual precipitation from the Daymet
MAP_worldclim	mm	mean annual precipitation from WorldClim
MAT_site	degree_C	mean annual temperature as reported by site personnel
MAT_daymet	degree_C	mean annual temperature from the Daymet
MAT_worldclim	degree_C	mean annual temperature from WorldClim
primary_veg_type	-	the dominant vegetation type at the site
secondary_veg	-	secondary vegetation type at the site
dominant_species	-	Latin binomials for the dominant species at each site, as reported by site personnel
landcover_igbp	-	numeric code corresponding to the land cover classification scheme of the International Geosphere-Biosphere Programme, derived from MODIS imagery (Friedl et al., 2010; Channan et al., 2014)
wwf_biome	-	numeric code corresponding to the biome classification scheme of the World Wildlife Fund (Olson et al., 2001)
koeppen_geiger	-	climate classification according to the Köppen-Geiger system (Kottek et al, 2006)
site_acknowledgments	-	data end users are asked to include this text, which has been provided by site collaborators, in publications and presentations that make use of data for this site

Region of interest (ROI) mask and ROI list

For each camera, a region of interest (ROI) was identified in the image scene that depicted a relatively uniform vegetation type. The "ROI

mask" file is a binary image mask in 8-bit TIF image format (*.tif) that identifies the pixels over which the image analysis was conducted. The black region of these TIF files denotes the ROI; white regions were excluded from calculations.

The “ROI list files” list the date and time range over which each binary image mask was applied in processing the image data for a site. With ROI mask and ROI list files, the data presented in the *_roistats.csv data files can be reproduced from the original image files.

In the ROI list files, the first 13 lines (beginning with #), document the provenance of the ROI list, and contain a brief description of the vegetation that is delineated by the associated image masks. Line 14 lists the column headers for the mask entry rows.

Table 3. Variables in the <**sitename**>_<**veg_type**>_<**ROI_ID**>_roi.csv files.

Variable	Units	Description
start_date	YYYY-MM-DD	date of the first image in the archive for this site
start_time	hh:mm:ss	time of capture of the first image for this site
end_date	YYYY-MM-DD	date of the most recent image as of the last_updated date. The date code "9999-12-31" was used to keep the processing open-ended
end_time	hh:mm:ss	time of capture of the most recent image for this site
mask_file	-	filename for the mask file with black for the ROI and white for pixel to exclude from calculations
sample_image	-	filename for a sample image in the date range

Table 4. Vegetation type abbreviations for ROIs (region of interests). With sites with multiple ROIs, each ROI contributed to the site-years value. Number of sites is the unique combination of ROI by site.

Abbreviation	Description	Site-years	Number of sites
AG	agriculture	703.5	161
DB	deciduous broadleaf	1185.2	171
DN	deciduous needleleaf	115.3	13
EB	evergreen broadleaf	101.8	22
EN	evergreen needleleaf	778	122
GR	grassland	912.4	188
MX	mixed vegetation	13.7	2
NV	non-vegetated	17.2	3
RF	non-vegetated	2.7	1
SH	shrubs	436.8	86
TN	tundra	117	20
UN	forest understory	219.2	41
WL	wetland	202.7	39
	Total	4805.5	869

ROI color statistics (*_roistats.csv)

These files contain the high-frequency (typically, 30 minute) color information extracted from the entire image archive for each site, using the ROI list files and ROI mask files. For each archived image, RGB (red, green, blue) color channel information was extracted for the ROI then means and other statistics were calculated for each channel. From the high-frequency (typically, 30 minute) imagery, time series characterizing vegetation color, including “canopy greenness” (Gcc), are included. The time series have not been filtered, and each data row in the file corresponds to an individual image in the archive.

In the files, the first 17 lines (beginning with #) contain basic metadata:

- Line 4 contains the sitename, identical to that in the filename.
- Lines 5 (veg_type) and 6 (ROI_ID_number) identify the vegetation type and the ROI_ID from the ROI list files.
- Lines 7-9 are site location (latitude and longitude in decimal degrees, and elevation in m above sea level.
- Line 10 is the UTC offset. [Lines 4-10 were extracted from the site metadata text files.]
- Line 11 indicates whether images have been re- resized to common dimensions (to match the size of the mask file) prior to analysis.
- Line 12 indicates the version of the data set.
- Lines 13-16 document the provenance of the data file.
- Line 18 lists the column headers for the data rows, and the data rows begin on line 19 with each data row corresponding to results for an individual image in the archive.

Table 5. Variables in the **<sitename>_<veg_type>_<ROI_ID>_roistats.csv** files.

Variable	Units	Description
date	YYYY-MM-DD	local date

local_std_time	hh:mm:ss	local standard time
doy	d	day of year
filename	-	image filename
solar_elev	degrees	solar elevation angle
exposure	-	image exposure
mask_index	1	mask number in the image mask sequence
gcc	1	mean green chromatic coordinate (Gcc) over the ROI
rcc	1	mean red chromatic coordinate (Rcc) over the ROI
r_mean	1	mean red channel digital number (DN) over the ROI
r_std	1	standard deviation (across pixels) of red channel DN over the ROI
b_mean	1	mean blue channel DN over the ROI
b_std	1	standard deviation (across pixels) of blue channel DN over the ROI
g_mean	1	mean green channel DN over the ROI
g_std	1	standard deviation (across pixels) of green channel DN over the ROI
r_5_qtl	1	the 5th quantile values (across pixels) of the red channel DN over the ROI
r_10_qtl	1	the 10th quantile values (across pixels) of the red channel DN over the ROI
r_25_qtl	1	the 25th quantile values (across pixels) of the red channel DN over the ROI
r_50_qtl	1	the 50th quantile values (across pixels) of the red channel DN over the ROI
r_75_qtl	1	the 75th quantile values (across pixels) of the red channel DN over the ROI
r_90_qtl	1	the 90th quantile values (across pixels) of the red channel DN over the ROI
r_95_qtl	1	the 95th quantile values (across pixels) of the red channel DN over the ROI
b_5_qtl	1	the 5th quantile values (across pixels) of the blue channel DN over the ROI
b_10_qtl	1	the 10th quantile values (across pixels) of the blue channel DN over the ROI
b_25_qtl	1	the 25th quantile values (across pixels) of the blue channel DN over the ROI
b_50_qtl	1	the 50th quantile values (across pixels) of the blue channel DN over the ROI
b_75_qtl	1	the 75th quantile values (across pixels) of the blue channel DN over the ROI
b_90_qtl	1	the 90th quantile values (across pixels) of the blue channel DN over the ROI
b_95_qtl	1	the 95th quantile values (across pixels) of the blue channel DN over the ROI
g_5_qtl	1	the 5th quantile values (across pixels) of the green channel DN over the ROI
g_10_qtl	1	the 10th quantile values (across pixels) of the green channel DN over the ROI
g_25_qtl	1	the 25th quantile values (across pixels) of the green channel DN over the ROI
g_50_qtl	1	the 50th quantile values (across pixels) of the green channel DN over the ROI
g_75_qtl	1	the 75th quantile values (across pixels) of the green channel DN over the ROI
g_90_qtl	1	the 90th quantile values (across pixels) of the green channel DN over the ROI
g_95_qtl	1	the 95th quantile values (across pixels) of the green channel DN over the ROI
r_g_cor	1	correlation coefficient (across pixels) between red channel DN and green channel DN, over the ROI
g_b_cor	1	correlation coefficient between green channel DN and blue channel DN, over the ROI
b_r_cor	1	correlation coefficient between blue channel DN and red channel DN, over the ROI

ROI color statistics: 1-day and 3-day summaries (*1_day.csv, *_3day.csv)

These files contain the daily summaries of time series data characterizing vegetation color, including “canopy greenness” for each site. From the high-frequency (typically, 30 minute) imagery, time series characterizing vegetation color, including “canopy greenness” was processed to 1-day intervals.

Although the latest date for acquired images is 2023-12-31, values for "smooth" variables may extend to 2024-03-03. These values were generated by interpolation using a smoothing function fitted to data from previous years; they are marked as interpolated by the *int_flag* variable.

For 1- day summary product files, the first 24 lines (beginning with #) contain basic metadata.

- Lines 4 through 10 are identical to those in *_roi.csv.

- Line 11 is not used in this dataset but allows for the specification of an image count threshold for processing to occur (i.e., if for a given period of aggregation, there are insufficient images available, then only results for the midday image, if applicable, would be reported).
- Line 12 gives the number of days that have been aggregated in producing the file" "1" for 1-day files; "3" for 3-day files.
- Line 13 reports the solar elevation filter that was used in processing (10° in the current data set).
- Lines 14 and 15 are not used in the data sets but allows for the specification of time-of-day window (i.e., images outside of the window would be excluded from the processing).
- Lines 16 and 17 report the values that were used for the “too dark” and “too bright” quality control filters, which are by default set to DN 100 and 665, respectively.
- Lines 18-23 document the provenance of the data file.
- Line 25 lists the column headers for the data rows, and the data begins on line 26..

Table 6. Variables in the <**sitename**>_<**veg_type**>_<**ROI_ID**>_1day.csv and <**sitename**>_<**veg_type**>_<**ROI_ID**>_3day.csv files.

Variable	Units	Description
date	YYYY-MM-DD	local date at the middle of the aggregation period (1-day)
year	YYYY	calendar year of the above date
doy	d	day of year for the above date
image_count	1	the number of images passing the selection criteria
midday_filename	-	the filename of the image which is closest to 12 noon
midday_r	1	mean red channel digital number (DN) over the ROI, for the midday image
midday_g	1	mean green channel DN over the ROI, for the midday image
midday_b	1	mean blue channel DN over the ROI, for the midday image
midday_gcc	1	the mean Gcc over the ROI, for the midday image
midday_rcc	1	the mean Rcc over the ROI, for the midday image
r_mean	1	the mean value (for all images passing the selection criteria) of the mean (by image) red channel DN over the ROI
r_std	1	the standard deviation (for all images passing the selection criteria) of the mean (by image) red channel DN over the ROI
g_mean	1	the mean value (for all images passing the selection criteria) of the mean (by image) green channel DN over the ROI
g_std	1	the standard deviation (for all images passing the selection criteria) of the mean (by image) green channel DN over the ROI
b_mean	1	the mean value (for all images passing the selection criteria) of the mean (by image) blue channel DN over the ROI
b_std	1	the standard deviation (for all images passing the selection criteria) of the mean (by image) blue channel DN over the ROI
gcc_mean	1	the mean value (for all images passing the selection criteria) of the mean (by image) Gcc over the ROI
gcc_std	1	the standard deviation (for all images passing the selection criteria) of the mean (by image) Gcc over the ROI
gcc_50, gcc_75, gcc_90	1	the 50th, 75th and 90th quantiles (for all images passing the selection criteria) of the mean (by image) Gcc over the ROI
rcc_mean, rcc_std, rcc_50, rcc_75, rcc_90	1	the 50th, 75th and 90th quantiles (for all images passing the selection criteria) of the mean (by image) RGcc over the ROI
max_solar_elev	degrees	the maximum solar elevation angle for all images passing the selection criteria
snowflag	1	not included in this release
outlierflag_gcc_mean, outlierflag_gcc_50; outlierflag_gcc_75, outlierflag_gcc_90	1	the outlierflag, which is determined separately for the gcc_mean, gcc_50, gcc_75, and gcc_90 time series, can either take on a value of 0 (indicating good data), or 1 (indicating an outlier)
smooth_gcc_mean, smooth_gcc_50, smooth_gcc_75, smooth_gcc_90	1	the smoothed and/or interpolated value of Gcc from the final iteration (i.e. with outliers removed) of the spline fitting process
smooth_rcc_mean, smooth_rcc_50, smooth_rcc_75, smooth_rcc_90	1	the smoothed and/or interpolated value of Rcc from the final iteration (i.e. with outliers removed) of the spline fitting process

smooth_ci_gcc_mean, smooth_ci_gcc_50, smooth_ci_gcc_75, smooth_ci_gcc_90	1	the (one-sided) width of the 95% confidence interval around the smoothed Gcc values
smooth_ci_rcc_mean, smooth_ci_rcc_50, smooth_ci_rcc_75, smooth_ci_rcc_90	1	the (one-sided) width of the 95% confidence interval around the smoothed Rcc values
int_flag	-	interpolation flag is set to "1" during a gap of 14 days or more; otherwise" NA"

Phenological transition dates

These files contain estimates of the transition date for the start of each “greenness rising” stage and end of each “greenness falling” stage, derived from the ROI color statistics 1-day and 3-day summary data.

File description for transition date files:

- The first 16 lines (beginning with #) contain basic metadata.
- Lines 4 through 6 are identical to those in the summary product file from which the transition date file is derived.
- Line 7 gives the number of days that have been aggregated in producing the file, which is either 1 day or 3 days.
- Lines 8 and 9 define the first and last years for which the transition dates are calculated.
- Lines 10 and 11 document the provenance of the data file.
- Lines 12-15 report goodness-of-fit statistics (in terms of RMSE, the root mean squared error) for the spline curves from which the transition dates are extracted.
- Line 17 lists the column headers for the data rows.
- The data rows begin on line 18. Each data row corresponds to a single “greenness rising” or “greenness falling” stage.

Table 7. Variables in <**sitename**>_<**veg_type**>_<**ROI_ID**>_1day_ transition_dates.csv and <**sitename**>_<**veg_type**>_<**ROI_ID**>_3day_transition_dates.csv files

Variable	Units	Description
sitename	-	the name of the camera site
veg_type	-	a two-letter abbreviation identifying the dominant vegetation within the ROI
roi_id	1	a numeric code (ROI_ID_number) to distinguish between multiple ROIs of the same vegetation type at a given site
direction	-	indicates whether the transition dates correspond to a “greenness rising” or “greenness falling” stage. Note: there may be more than one rising/falling cycle per calendar year, and a single rising or falling stage may cut across years.
gcc_value		indicates the variable used to calculate transition dates: gcc_mean, gcc_50, gcc_75 or gcc_90 time series
transition_10, transition_25, transition_50	YYYY-MM-DD	transition dates for each “greenness rising” or “greenness falling” stage, corresponding to 10%, 25% and 50% of the Gcc amplitude of that stage
transition_10_lower_ci, transition_25_lower_ci, transition_50_lower_ci, transition_10_upper_ci, transition_25_upper_ci, transition_50_upper_ci	YYYY-MM-DD	dates corresponding to the lower and upper 95% confidence intervals on the 10%, 25%, and 50% of the Gcc amplitude
threshold_10, threshold_25, threshold_50	1	the threshold values of Gcc used to identify transition dates
min_gcc, max_gcc	1	the baseline (dormant-season minimum) and peak (active-season maximum) Gcc values, calculated from the fitted spline, as used to derive the Gcc amplitude

Camera NDVI statistics (*_ndvi_roistats.csv, *_ndvi_1day.csv, * _ndvi_3day.csv)

These data files contain derived data and metadata used to calculate *cameraNDVI*. There are two distinct data file types.
The <site_name>_<vegetation_type>_<ROI>_ndvi_roistats.csv files hold statistics for PhenoCam Camera NDVI ROI (RGB/IR Image Pair).
The <site_name>_<vegetation_type>_<ROI>_ndvi_1day.csv (or *_ndvi_3day.csv) files hold 1-day and 3-day NDVI summaries.

The “image pair statistics files,” the files are formatted as follows.

- The first 17 lines (beginning with #) contain basic metadata:
- Line 4 contains the sitename, identical to that in the filename.
- Lines 5 (veg_type) and 6 (ROI_ID_number) identify the vegetation type and the ROI_ID from the ROI list files.
- Lines 7-9 are site location (latitude and longitude in decimal degrees, and elevation in m above sea level.
- Line 10 is the UTC offset. [Lines 4-10 were extracted from the site metadata text files.]
- Line 11 indicates whether images have been re- resized to common dimensions (to match the size of the mask file) prior to analysis.
- Line 12 indicates the version of the data set.
- Lines 13-16 document the provenance of the data file.

- Line 18 lists the column headers for the data rows.
- The data begin on line 19 with each data row corresponding to results for a specific pair of RGB and RGB+IR in the archive.

Table 8. Variables in the <**site_name**>_<**veg_type**>_<**ROI**>_ndvi_roistats.csv

Variable	Units	Description
date	YYYY-MM-DD	local date for image
local_std_time	hh:mm:ss	local standard time
doy	1	day of year
filename_rgb	-	RGB filename
filename_ir	-	IR filename
solar_elev	degrees	solar elevation angle
exposure_rgb	1	exposure of RGB image
exposure_ir	1	exposure of IR image
mask_index	1	index into mask list
r_mean	1	mean red digital number (DN) over the ROI
g_mean	1	mean green DN over the ROI
b_mean	1	mean blue DN over the ROI
ir_mean	1	mean DN over the ROI from the IR image
ir_std	1	standard deviation of DN over the ROI from the IR image
ir_5_qtl, ir_10_qtl, ⋯, ir_90_qtl, ir_95_qtl	1	the 5, 10,..., 90, 95 quantile values of the DN values over the ROI
Y, Z_prime, R_prime, Y_prime, X_prime	1	intermediate values for camera NDVI calculation
NDVI_c	1	camera NDVI as calculated in Petach et al. (2014)

For the "1-day and 3-day NDVI Summary Files", the files are formatted as follows.

- Lines 4 through 10 are identical to those in the all-image time series file from which the summary product files are derived.
- Line 11 is not used in the data sets but allows for the specification of an image count threshold for processing to occur (i.e., if for a given period of aggregation, there are insufficient images available, then only results for the midday image, if applicable, would be reported).
- Line 12 gives the number of days that have been aggregated in producing the file, which is 1 or 3 days.
- Line 13 reports the solar elevation filter that was used in processing (10° in the current data set).
- Lines 14 and 15 are not used in the data sets but allows for the specification of time-of-day window (i.e., images outside of the window would be excluded from the processing).
- Lines 16 and 17 report the values that were used for the "too dark" and "too bright" quality control filters, which are by default set to DN 100 and 665, respectively.
- Lines 18-21 document the provenance of the data file.
- Line 23 lists the column headers for the data rows, and the data rows begin on line 24.

Table 9. Variables in the *<**site_name**>_<**veg_type**>_<**ROI**>_ndvi_1day.csv* or **_ndvi_3day.csv* files.

Variable	Units	Description
date	YYYY-MM-DD	local date of middle of aggregation period (1-day or 3-day)
doy	d	doy for this date
image_count	1	number of images passing the selection criteria
midday_rgb_filename	-	filename for the RGB image which is closest to noon (midday image) on the middle day of summary period
midday_ir_filename	-	filename for the IR image which is closest to noon (midday image) on the middle day of summary period
midday_ndvi	1	mean NDVI over ROI for the midday image
gcc_90	1	90th percentile Gcc value for all the image pairs passing the selection criteria
ndvi_mean	1	mean NDVI value for all the image pairs passing the selection criteria
ndvi_std	1	standard deviation of NDVI values for all the image pairs passing the selection criteria
ndvi_50, ndvi_75, ndvi_90	1	50th, 75th, and 90th percentiles of NDVI values
max_solar_elev	degrees	maximum solar elevation for the images from this day
snow_flag	-	not included in this release
outlierflag_ndvi_mean	-	outlier flag for NDVI mean value (1=outlier) [not included in this release]

outlierflag_ndvi_50	-	outlier flag for NDVI 50th percentile value (1=outlier) [not included in this release]
outlierflag_ndvi_75	-	outlier flag for NDVI 75th percentile value (1=outlier) [not included in this release]
outlierflag_ndvi_90	-	outlier flag for NDVI 90th percentile value (1=outlier) [not included in this release]

Simplified data files

These data files contain highly simplified data and derived data products. There are two file types in this data record: The <sitename>_<veg_type>_ROI_ID_number>_simplified_1day.csv files are "Simplified Daily Summary Files" that report the aggregated statistics for G_{cc}_mean at a 1-day aggregation period.

The <sitename>_<veg_type>_ROI_ID_number>_simplified_transition_dates.csv) are "Simplified Transition Date Files" that report transition dates for G_{cc}_mean, extracted from the 1-day transition dates. Unlike other data records, the simplified data records do not include metadata, and data are only reported 1-day time step.

Table 10. Variables in the <**sitename**>_<**veg_type**>_<**ROI_ID**r>_simplified_1day.csv files.

Variable	Units	Description
date	YYYY-MM-DD	local date
gcc_mean	1	mean daily Gcc value from <site>_*_1day.csv file
smooth_gcc_mean	1	smoothed value of Gcc from the optimized spline, from <site>_*_1day.csv file

Table 11. Variables in the <**sitename**>_<**veg_type**>_<**ROI_ID**>_simplified_transition_dates.csv files.

Variable	Units	Description
year	YYYY	year in which the transition occurred (YYYY)
direction	-	indicates whether the date corresponds to a “greenness rising” or “greenness falling” stage. Note: there may be more than one rising/falling cycle per calendar year, and a single rising or falling stage may cut across years.
date_10, date_25, date_50	YYYY-MM-DD	transition dates for each “greenness rising” or “greenness falling” stage, corresponding to 10%, 25% and 50% of the Gcc amplitude of that stage.
DOY_10, DOY_25, DOY_50	d	day-of-year values corresponding to the calendar date transitions

PhenoCam site locations

The locations of PhenoCam sites are included as point locations in a GeoJSON file: *phenocam_sites_v3.geojson.* Site locations are duplicated if there are >1 ROI at the site.

Table 12: Point attributes for PhenoCam locations in *phenocam_sites_v3.geojson.*

Attribute	Units	Description
sitename	-	name of the camera site, e.g. “coweeta,” used to designate all images and products associated with that site
veg_type	-	dominant vegetation type for the ROI
roi_id	-	unique identifier to distinguish between multiple ROIs of the same vegetation type for a given site
start_date	YYYY-MM-DD	the date of the first image in the archive for this site
end_date	YYYY-MM-DD	the date of the most recent image as of the last_updated date
days	d	cumulative number of days of activity
site_years	y	number of years of activity
description	-	description of site conditions
ecoregion	-	numeric code identifying the site’s EPA Ecoregion
koeppen_geiger	-	climate classification according to the Köppen-Geiger system (Kottek et al, 2006)
landcover_igbp	-	numeric code corresponding to the land cover classification scheme of the International Geosphere-Biosphere Programme (Friedl et al., 2010; Channan et al., 2014)
elev	m	elevation of the ground surface (m above sea level) at the camera site
MAT_site	degree_C	mean annual temperature as reported by site personnel
MAP_site	mm	mean annual precipitation as reported by site personnel
lat	degrees_north	the latitude (in decimal degrees) of the camera itself

lon	degrees_east	the longitude (in decimal degrees) of the camera itself

3. Application and Derivation

Data derived from PhenoCam imageries can be used for phenological model validation and development, evaluation of satellite remote sensing data products, understanding relationships between canopy phenology and ecosystem processes, studies of the seasonal changes in leaf-level physiology associated with changes in leaf color, benchmarking earth system models, and studies of climate change impacts on terrestrial ecosystems (Richardson et al., 2018).

4. Quality Assessment

Quality assurance was conducted by quantitative analysis through automated quality control routines (e.g. filtering and outlier detection) and a visual evaluation of each time series to examine consistency and overall quality (Richardson et al., 2018; Seyednasrollah et al. 2019; Young et al., 2024).

5. Data Acquisition, Materials, and Methods

PhenoCam Network

The PhenoCam network is a cooperative network, established in 2008 and uses digital camera imagery to monitor ecosystem dynamics over time. It serves as a long-term, continental-scale, phenological observatory with cameras deployed within North America, Europe, and other continents. This dataset includes sites from 30 countries (Figure 2).

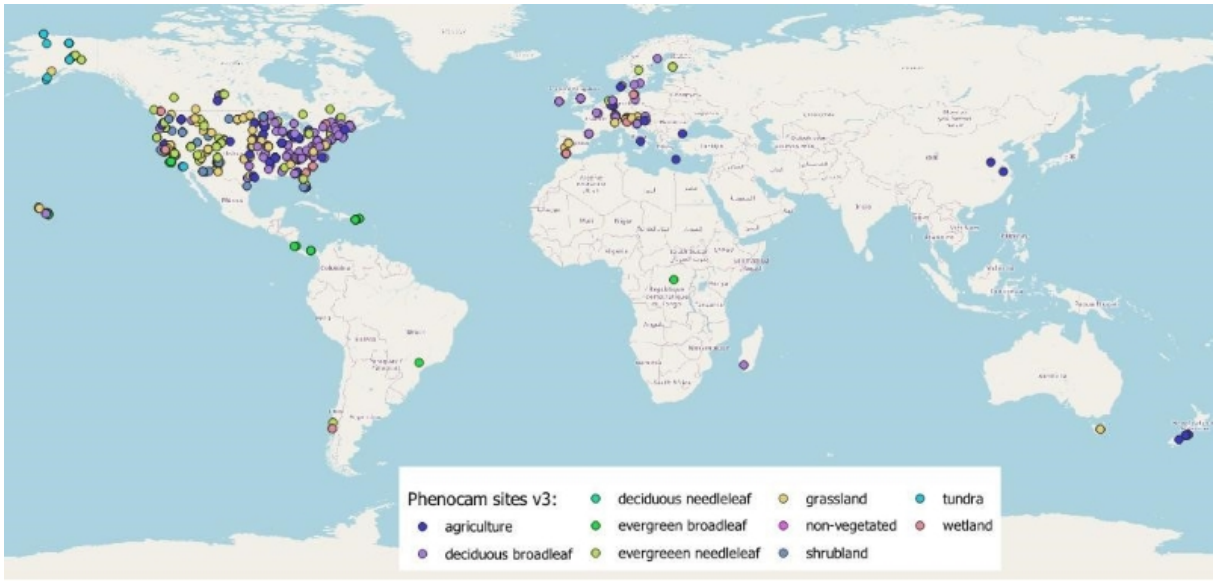

Figure 2. Global distribution of PhenoCam sites represented in this dataset. There are 638 sites in North America, 85 in Europe, 7 in Oceania, 4 in South America, 2 in Africa, and 2 in Asia.

This dataset was derived from conventional, visible-wavelength, automated digital camera imagery from 738 camera sites, together totaling 4805.5 years of data across different ecoregions, climate zones, and vegetation types. Vegetation types such as deciduous broadleaf forests, grasslands, evergreen needleleaf forests, and agriculture are the best-represented (Table 4). Raw imagery is available in Ballou et al. (2024).

For each archived image, summary statistics for RGB (red, green, blue) color channels were calculated across a region-of-interest (ROI) delineating a specific vegetation type. From the high-frequency (typically, 30 minute) imagery, time series characterizing vegetation color, including canopy greenness (canopy greenness index -- the green chromatic coordinate, Gcc) and red chromatic coordinate (Rcc) were derived for 1- and 3-day intervals. For ecosystems with one or more annual cycles of vegetation activity, the start of the “greenness rising” and end of the “greenness falling” stages is provided. A “cameraNDVI” time series was derived from visible and visible+NIR imagery collected from the majority of cameras (see Petach et al., 2014). In addition, a new set of simplified data products are included that will be easier for most users to use (see Young et al., 2024).

Every night, any new images uploaded to the PhenoCam data server during the previous 24 hours were processed and analysed as described in Richardson et al. (2018).

Image analysis and data processing

Image analysis consists of several steps. First, an appropriate “region of interest” (ROI) is defined, corresponding to the area within each digital image for which color information will be extracted (e.g., Figure 1). The ROIs characterize the dominant vegetation type in that portion of each image. For sites where more than one vegetation type could be clearly identified, secondary ROIs are selected. The ROI coordinate definitions were stored, in TIFF format, as a series of binary image masks, which comprise an ROI’s “mask sequence”. For each ROI mask sequence at each site, an “ROI list” file details the date and time range over which each mask was applied.

The digital cameras recorded JPEG images with color information stored in three separate layers (red, green, and blue; RGB). According to the standard additive color model, representation of any given color in the visible range is achieved by varying the intensity (pixel value) of these primary colors. Thus, each pixel in the image is associated with a digital number (“DN”) triplet, with each element in the triplet corresponding to the intensity of one of the three color layers. Therefore, the second step in the image analysis was to read in the images and associated mask sequence, and to characterize the frequency distribution of the RGB DN triplets across the mask. This second step was done separately for each ROI at each site, to produce the “ROI color statistics” time series data files.

The frequency distribution of the RGB DN triplets across the mask was characterized on a channel-by-channel basis, and also in terms of the

pairwise correlation of DN values between color channels. Thus, for each of the red, green and blue color channels, the mean and standard deviation, as well as the 5th, 10th, 25th, 50th, 75th, 90th, and 95th quantiles, of the DN distribution across all pixels in the ROI was determined. Similarly, distributional statistics were calculated for Gcc and Rcc.

For each image, the date and local time were extracted from the image file name. In addition, the solar elevation angle based on the date and local time stamp, using standard formulas was calculated.

The Complementary Metal Oxide Semiconductor (CMOS) imaging sensor within network-enabled digital cameras is sensitive to near infrared (NIR) wavelengths, and the cut filter used to block wavelengths ≥700 nm for standard visible-wavelength (RGB) images is software controlled. With the filter removed, the camera records an RGB+NIR image (Petach et al., 2014). The original intent of this design was to enhance photon capture under low-light conditions and to permit nighttime security monitoring with an infrared illuminator. However, it has the potential for the camera to serve as a four-channel imager (red, green, blue, and NIR) — enabling calculation of a "camera NDVI" (normalized difference vegetation index) from digital numbers and exposure values (Petach et al 2014), similar to the standard NDVI calculated using reflectances. For additional information, see Young et al. (2024).

Transition Date Estimation

Using an approach similar to the "spline interpolation" method that has been previously applied to PhenoCam data, phenophase transition dates for each ROI mask sequence were extracted. These were intended to define the start of the "greenness rising" and end of the "greenness falling" stage for a full cycle of vegetation activity (i.e., from dormancy, through green-up or "greenness rising", peak activity, senescence or "greenness falling", and back to dormancy). The transition dates are reported only for the Gcc time series and not for *camera NDVI.*

See Richardson et al. (2018) and Young et al. (2024) for more details about the PhenoCam project and related analyses.

6. Data Access

These data are available through the Oak Ridge National Laboratory (ORNL) Distributed Active Archive Center (DAAC).

PhenoCam Dataset v3.0: Vegetation Phenology from Digital Camera Imagery, 2000-2023

Contact for Data Center Access Information:

- E-mail: uso@daac.ornl.gov
- Telephone: +1 (865) 241-3952

7. References

Ballou, K., Z. Vladich, A.M. Young, T. Milliman, K. Hufkens, C. Coffey, K. Begay, M. Fell, M. Javadian, A.K. Post, C. Schadel, O. Zimmerman, D.M. Browning, C.R. Florian, M.A. Friedl, M. Moon, M.D. SanClements, B. Seyednasrollah, A.D. Richardson, M. Abraha, D.W. Allen, M. Apple, M.A. Arain, A.C. Axel, P.H.J. Badiou, M. Bahn, J. Baker, D. Baldocchi, S.L.J. Bayliss, N. Behrens, C.M. Beier, C.J. Bernacchi, D. Berveiller, J. Bhattacharjee, S.C. Biraud, J.J. Blais, P. Blanken, M. Bonfim, D.D. Bosch, R. Boughton, E.H. Boughton, R.F. Brown, N. Brunsell, S.P. Burns, M.S. Carbone, B.R. Carlson, A. Carrara, M. Cavagna, W.S. Chan, J. Chen, A. Christen, N. Chrysoulakis, H. Chu, P.E. Clark, B.J. Conrad, M.R. Cortese, R.M. Crandall, E. Cremonese, H. Crepaz, F.W. Davis, D. Debinski, A.R. Desai, M. Detto, R. Diaz-Delgado, L. Duchesne, A.L. Dunn, K.J. Easterday, D.M. Eissenstat, T. El-Madany, D.S.S. Ellum, S.K.M. Ernest, A. Esposito, E.S. Euskirchen, L. Fenstermaker, L.F. Filchev, J.M. Fill, L.B. Flanagan, B. Forsythe, J.M. Frank, A.L. Freestone, J. Gallagher, M.B. Garcia, D. Garcia-diaz, M. Gharun, D. Gianelle, J.M. Gonet, S.C. Goslee, T. Griffis, P. Groffman, L. Gu, J. Guillemot, I.M. Halm, M. Halpin, A. Hammerle, C.V. Hanson, P.J. Hanson, Z. Harlow, K.M. Hart, C.E. Hatch, P.L. Heinrich, D. Hemming, M. Heskel, A.C. Hill, A.A. Hove, T. Hubner, D. Hui, E.R. Humphreys, P.C. Inkenbrandt, A. Jaimes-Hernandez, R. Jensen, B.G. Johnson, J.M.F. Johnson, L.S.K. Joseph, E. Keel, V.R. Kelly, K.W. King, J.W. Kirchner, P.B. Kirchner, M.A. Kline, S.H. Knox, M. Krassovski, K.L. Ladig, P.E. Laerke, O. Langvall, N.K. Lany, G. Lanthier, G. le Maire, H. Liu, Y.P. Luo, R.L. JimÃ©nez, A. Manco, J. Marrs, T.A. Martin, M. Mauritz, G. McCarty, B. McNeil, F. Meier, M. Mensinger, G.A. Meyer, M. Migliavacca, T. Miura, B.P. Mohanty, C.E. Moore, R. Mudd, J.W. Munger, Z.E. Murrell, Z. Nesic, H.S. Neufeld, J. Norris, J. O'Connell, T.L. O'Halloran, W. Oechel, A.C. Oishi, B. Oryan, W.W. Oswald, D.M.P. Peltier, J. Perez-Quezada, T.D. Perkins, C. Phillips, M. Pizarro, D. Poursanidis, J.W.M. Pullens, P. Ramanamandimby, M.P. Rao, R.L. Ray, M.L. Reba, C. Redmond, A. Reinmann, D.A. Roberts, G.P. Robertson, M. Rodriguez-Caton, K. Rumora, B.C. Rundquist, B.R.K. Runkle, T. Sachs, E.J. Sadler, A. Saha, N.Z. Saliendra, T.S. Sankey, H. Scheifinger, L. Schmalbeck, M.R. Schuppenhauer, M.D. Schwartz, R.L. Scott, S.D. Sebestyen, D. Smale, E.M. Smith, J. Smith, O. Sonnentag, P. Stoy, S. Strachan, K. Suvocarev, D. Szutu, F. Tekinay, J.E. Thom, R.Q. Thomas, C. Trauernicht, D. Trejo, D. Tsirantonakis, A. Valero, A.K. Van den berg, M.K. Van der molen, R. Vargas, M. Vellend, J. Verfaillie, C.S. Vogel, A. Vrieling, J.J. Walker, J.R. Ward, D.A. Watts, N. Webb, P. Wetzel, S. Weyers, A.V. Whipple, C.W. Whippo, W.A. White, T.G. Whitham, C. Wille, A. Wingler, G. Wohlfahrt, S. Wolf, J.D. Wood, A.L. Woodley, J. Yang, X. Yang, G. Yenni, A.J. Zambrano-olimpo, A. Zandonai, Y. Zhang, and D. Zona. 2025. PhenoCam Dataset v3.0: Digital Camera Imagery from the PhenoCam Network, 2000-2023. ORNL DAAC, Oak Ridge, Tennessee, USA. https://doi.org/10.3334/ORNLDAAC/2364

Channan, S., K. Collins, and W.R. Emanuel. 2014. Global mosaics of the standard MODIS land cover type data. University of Maryland and the Pacific Northwest National Laboratory, College Park, Maryland, USA<, 30.

Friedl, M.A., D. Sulla-Menashe, B. Tan, A. Schneider, N. Ramankutty, A. Sibley, and X. Huang. 2010. MODIS Collection 5 global land cover: Algorithm refinements and characterization of new datasets. Remote Sensing of Environment 114:168-182. https://doi.org/10.1016/j.rse.2009.08.016

Kottek, M., Grieser, J., Beck, C., Rudolf, B. and Rubel, F., 2006. World map of the Köppen-Geiger climate classification updated. Meteorologische Zeitschrift 15:259-263. https://doi.org/10.1127/0941-2948/2006/0130

Milliman, T., B. Seyednasrollah, A.M. Young, K. Hufkens, M.A. Friedl, S. Frolking, A.D. Richardson, M. Abraha, D.W. Allen, M. Apple, M.A. Arain, J.M. Baker, D. Baldocchi, C.J. Bernacchi, J. Bhattacharjee, P. Blanken, D.D. Bosch, R. Boughton, E.H. Boughton, R.F. Brown, D.M. Browning, N. Brunsell, S.P. Burns, M. Cavagna, H. Chu, P.E. Clark, B.J. Conrad, E. Cremonese, D. Debinski, A.R. Desai, R. Diaz-Delgado, L. Duchesne, A.L. Dunn, D.M. Eissenstat, T. El-Madany, D.S.S. Ellum, S.M. Ernest, A. Esposito, L. Fenstermaker, L.B. Flanagan, B. Forsythe, J. Gallagher, D. Gianelle, T. Griffis, P. Groffman, L. Gu, J. Guillemot, M. Halpin, P.J. Hanson, D. Hemming, A.A. Hove, E.R. Humphreys, A. Jaimes-Hernandez, A.A. Jaradat, J. Johnson, E. Keel, V.R. Kelly, J.W. Kirchner, P.B. Kirchner, M. Knapp, M. Krassovski, O. Langvall, G. Lanthier, G.l. Maire, E. Magliulo, T.A. Martin, B. McNeil, G.A. Meyer, M. Migliavacca, B.P. Mohanty, C.E. Moore, R. Mudd, J.W. Munger, Z.E. Murrell, Z. Nesic, H.S. Neufeld, W. Oechel, A.C. Oishi, W.W. Oswald, T.D. Perkins, M.L. Reba, B. Rundquist, B.R. Runkle, E.S. Russell, E.J. Sadler, A. Saha, N.Z. Saliendra, L. Schmalbeck, M.D. Schwartz, R.L. Scott, E.M. Smith, O. Sonnentag, P. Stoy, S. Strachan, K. Suvocarev, J.E. Thom, R.Q. Thomas, A.K. Van den berg, R. Vargas, J. Verfaillie, C.S. Vogel, J.J. Walker, N. Webb, P. Wetzel, S. Weyers, A.V. Whipple, T.G. Whitham, G. Wohlfahrt, J.D. Wood, J. Yang, X. Yang, G. Yenni, Y. Zhang, Q. Zhang, and D. Zona. 2019. PhenoCam Dataset v2.0: Digital Camera Imagery from the PhenoCam Network, 2000-2018. ORNL DAAC, Oak Ridge, Tennessee, USA. https://doi.org/10.3334/ORNLDAAC/1689

Olson, D.M., E. Dinerstein, E.D. Wikramanayake, N.D. Burgess, G.V. Powell, E.C. Underwood, J.A. D'amico, I. Itoua, H.E. Strand, J.C. Morrison, and C.J. Loucks. 2001. Terrestrial Ecoregions of the World: A New Map of Life on Earth: A new global map of terrestrial ecoregions provides an innovative tool for conserving biodiversity. BioScience 51:933-938. https://doi.org/10.1641/0006-3568(2001)051[0933:TEOTWA]2.0.CO;2

Petach, A.R., M. Toomey, D.M. Aubrecht, and A.D. Richardson. 2014. Monitoring vegetation phenology using an infrared-enabled security camera. Agricultural and Forest Meteorology 195–196:143-151. https://doi.org/10.1016/j.agrformet.2014.05.008

Richardson, A.D., K. Hufkens, T. Milliman, D.M. Aubrecht, M. Chen, J.M. Gray, M. R. Johnston, T.F. Keenan, S.T. Klosterman, M. Kosmala, E.K. Melaas, M.A. Friedl, and S. Frolking. 2018. Tracking vegetation phenology across diverse North American biomes using PhenoCam imagery. Scientific Data 5:180028. https://doi.org/10.1038/sdata.2018.28

Seyednasrollah, B., A.M. Young, K. Hufkens, T. Milliman, M.A. Friedl, S. Frolking, and A.D. Richardson. 2019a. Tracking vegetation phenology across diverse biomes using PhenoCam imagery: The PhenoCam Dataset v2.0. Scientific Data 6:222. https://doi.org/10.1038/s41597-019-0229-9

Seyednasrollah, B., A.M. Young, K. Hufkens, T. Milliman, M.A. Friedl, S. Frolking, A.D. Richardson, M. Abraha, D.W. Allen, M. Apple, M.A. Arain, J. Baker, J.M. Baker, D. Baldocchi, C.J. Bernacchi, J. Bhattacharjee, P. Blanken, D.D. Bosch, R. Boughton, E.H. Boughton, R.F. Brown, D.M. Browning, N. Brunsell, S.P. Burns, M. Cavagna, H. Chu, P.E. Clark, B.J. Conrad, E. Cremonese, D. Debinski, A.R. Desai, R. Diaz-Delgado, L. Duchesne, A.L. Dunn, D.M. Eissenstat, T. El-Madany, D.S.S. Ellum, S.M. Ernest, A. Esposito, L. Fenstermaker, L.B. Flanagan, B. Forsythe, J. Gallagher, D. Gianelle, T. Griffis, P. Groffman, L. Gu, J. Guillemot, M. Halpin, P.J. Hanson, D. Hemming, A.A. Hove, E.R. Humphreys, A. Jaimes-Hernandez, A.A. Jaradat, J. Johnson, E. Keel, V.R. Kelly, J.W. Kirchner, P.B. Kirchner, M. Knapp, M. Krassovski, O. Langvall, G. Lanthier, G.l. Maire, E. Magliulo, T.A. Martin, B. McNeil, G.A. Meyer, M. Migliavacca, B.P. Mohanty, C.E. Moore, R. Mudd, J.W. Munger, Z.E. Murrell, Z. Nesic, H.S. Neufeld, T.L. O'Halloran, W. Oechel, A.C. Oishi, W.W. Oswald, T.D. Perkins, M.L. Reba, B. Rundquist, B.R. Runkle, E.S. Russell, E.J. Sadler, A. Saha, N.Z. Saliendra, L. Schmalbeck, M.D. Schwartz, R.L. Scott, E.M. Smith, O. Sonnentag, P. Stoy, S. Strachan, K. Suvocarev, J.E. Thom, R.Q. Thomas, A.K. Van den berg, R. Vargas, J. Verfaillie, C.S. Vogel, J.J. Walker, N. Webb, P. Wetzel, S. Weyers, A.V. Whipple, T.G. Whitham, G. Wohlfahrt, J.D. Wood, S. Wolf, J. Yang, X. Yang, G. Yenni, Y. Zhang, Q. Zhang, and D. Zona. 2019b. PhenoCam Dataset v2.0: Vegetation Phenology from Digital Camera Imagery, 2000-2018. ORNL DAAC, Oak Ridge, Tennessee, USA. https://doi.org/10.3334/ORNLDAAC/1674

Young, A.M., T. Milliman, K. Hufkens, K. Ballou, C. Coffey, K. Begay, M. Fell, M. Javadian, A.K. Post, C. Schädel, Z. Vladich, O. Zimmerman, D.M. Browning, C.R. Florian, M.A. Friedl, M. Moon, M.D. SanClements, B. Seyednasrollah, and A.D. Richardson. 2024. Tracking vegetation phenology across diverse biomes using PhenoCam imagery: The PhenoCam Dataset v3.0. Submitted to *Earth System Science Data*.

8. Dataset Revisions

Version	Release Date	Revision Notes
3	2024-03-10	Time series extended to 2023. Total sites increased to 738 across global distribution. Added a new set of simplified data products and the Camera NDVI statistics.
2	2019-09-04	Time series was extended to 2018. Number of sites increased from 133 to 393. https://doi.org/10.3334/ORNLDAAC/1674.
1	2017-12-27	Original publication: https://doi.org/10.3334/ORNLDAAC/1511